Higher-order Ring Resonators and Delayed Interferometers Based on 300-mm SOI Technology for WDM Applications

Seok-Hwan Jeong, Yu Tanaka, and Ken Morito
Photonics Electronics Technology Research Association (PETRA)
AIST West-7SCR, 16-1 Onogawa, Tsukuba, Ibaraki 305-8569, Japan

Abstract— We introduce high-performance Si-nanowire WDM devices based on higher-order coupled resonator optical waveguides (CROW) and multi-stage delayed Mach-Zehnder interferometers (DMZI) fabricated by 300-mm SOI wafer-scale ArF-immersion lithography process. For the two kinds of WDM devices, we experimentally demonstrate low insertion loss, spectral flatness and low crosstalk properties, together with high manufacturing tolerances.

1. INTRODUCTION

Recently, total bandwidth per central processing unit in high-performance servers reaches to a few Tbit/s, which requires advanced optical interconnect technologies based on Si photonics to surpass the limits of transmission bandwidth and power consumption by electric wirings [1]. Wavelength division multiplexing (WDM) would be one of promising technologies to enhance the aggregate bandwidth and to reduce the assembly cost for connecting to optical fibers [2]. WDM optical interconnect normally requires Si-nanowire optical multiplexers/demultiplexers (MUX/DeMUX), from the viewpoint of monolithic integration with compact and energy-efficient Si-nanowire optical modulators and photo-detectors [3]. In almost cases, WDM devices work with the help of the lightwave interference based on the splitting and remixing at multiple optical paths. Thus, their operational performances strongly depend on the controllability of the relative phase relation between all of the optical paths [4, 5]. The phase controllability is mainly determined by the sidewall roughness of Si-nanowire waveguides. 300-mm silicon-on-insulator (SOI) wafer-scale ArF-immersion lithography technologies could be attractive for markedly reducing the phase errors in Si-nanowire waveguides [6]. Here, we report high-performance Si-nanowire waveguide based WDM devices such as higher-order coupled resonator optical waveguides (CROW) and multi-stage delayed Mach-Zehnder interferometer (DMZI) demultiplexers fabricated by phase controllable and highly productive 300-mm silicon-on-insulator (SOI) wafer-scale ArF-immersion lithography process [7, 8]. For the two kinds of WDM devices, we experimentally demonstrate low insertion loss, spectral flatness and low crosstalk properties, together with high manufacturing tolerances.

2. FIFTH-ORDER MICRORING RESONATORS

As a feasibility study of ArF-immersion lithography technology, we designed and fabricated Si-nanowire 5th-order CROW and characterized their spectral characteristics and spectral uniformities on a 300-mm SOI wafer. We demonstrated flat-topped spectral response with an excess loss of only 0.4 ± 0.2 dB and a high out-of-band rejection ratio of > 40 dB. Additionally, good spectral uniformities in intra-dies and inter-dies were achieved.

The 5th-order CROWs were fabricated on a 300-mm SOI wafer with a 0.22-μm-thick Si core layer and a 2-μm-thick buried oxide layer through ArF-immersion lithography process in National Institute of Advanced Industrial Science and Technology. Fig. 1 shows the top views of the fabricated 5th-order CROW based on 440-nm-wide Si-nanowire channel waveguides. Total chip area was 50 μm (width) ×150 μm (length).

Then, the fabricated 5th-order CROW devices were characterized with a linearly polarized TE-mode light. Fig. 2 shows the superimposed measured spectra in intra-dies uniformly spaced by 50-μm (a) and in inter-dies spaced by ~ 3 cm on a 300-mm SOI wafer (b). For both cases, clear flat-topped box-like spectral response was obtained by virtue of good phase controllability based on ArF-immersion lithography process. In Fig. 2(a), the standard deviation of phase variation was analyzed to be $\sim 0.03\pi$ radian for the optical path length of each microring. In Fig. 2(b), the center wavelength deviation was less than 3.6 nm, although the tested dies were separated by ~ 18 cm (distance between D2 and D8).

Spectral superiority over the ArF-immersion lithography process was reconfirmed by evaluating the eye diagrams of 25 Gbps non-return to zero (NRZ) modulation signals [7]. Dynamic signal

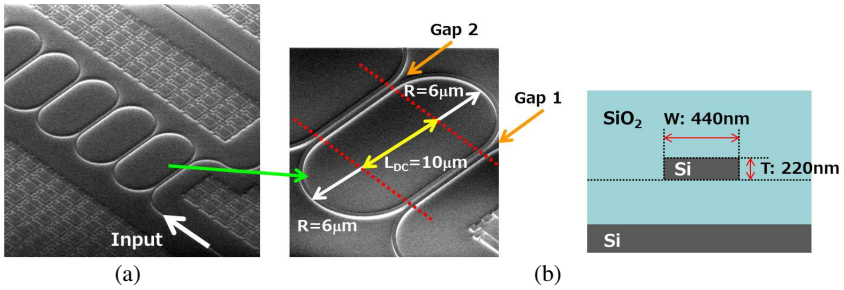

Figure 1: (a) Top views of the fabricated Si-nanowire based 5th-order CROW and (b) its schematic cross-sectional view of the waveguide with 440-nm-width and 220-nm-thickness.

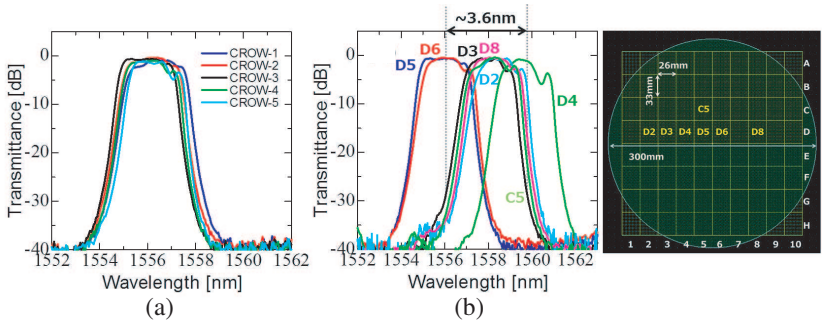

Figure 2: Measured spectra of the fabricated 5th-order CROWs, (a) intra-die distribution and (b) inter-die distribution.

waveforms were characterized by sending 25 Gbps NRZ modulation signals to the device. As a result, 25 Gbps modulation signal transmission was successfully implemented within almost passband wavelength range of the fabricated 5th-order CROW, which originated from the marked reduction of spectral ripple and low excess loss. This high-precision fabrication technology could also be applied to further advanced WDM DeMUX schemes. For example, by cascade-connecting such higher-order CROWs where filtering wavelengths for each microring are properly adjusted not to be overlapped with each other, optical DeMUX functionality could be achieved.

3. DELAYED-INTERFEROMETER-BASED OPTICAL MUX/DEMUX

Among several kinds of optical MUX/DeMUX, the DMZI-type devices [9–11] have a lot of advantages. Compared with higher-order CROW or arrayed waveguide grating (AWG), the DMZI-type device exhibits, in principle, much better spectral flatness that is one of important factors for relaxing the wavelength control accuracy of optical signal, without sacrificing insertion loss. Moreover, since the DMZI-type device can be formed with Si-nanowire channel waveguides only and does not need shallowly etched waveguide regions that are normally required to minimize scattering losses at around star couplers in AWG, fabrication process can be much simpler [10, 11]. Fig. 3 shows the device configuration of 1×4Ch multistage DMZI-based optical DeMUX (a) and the measured spectra of the fabricated DMZI DeMUX with the channel spacing ($\Delta\nu$) of 10 nm (b) and 6.4 nm (c). As shown in Fig. 3(a), the fabricated device is composed of cascade-connected 21 delayed interferometers with different optical path lengths at each stage [8, 11].

In general, in order to spatially discriminate four different wavelength components, the device configuration can be much simpler. Cascade-connecting only 3 delayed interferometers can make 1×4Ch optical DeMUX as already reported in [8, 9]. But, in that case, such device normally exhibits *sinc*-function-shaped spectra. Thus, its spectral performance becomes inferior in term of spectral flatness and low spectral crosstalk. These drawbacks can be overcome by introducing the device configuration shown in Fig. 3(a). Redundant delayed interferometers with different optical path lengths and optimized coupling ratios at each optical coupler make the optical DeMUX response spectrally flat and low crosstalk, maintaining low insertion loss. However, it should be noted that total phase errors becomes further higher than the case of the aforementioned simple device scheme, since the configuration shown in Fig. 3(a) inevitably needs much larger number of DMZIs with relatively longer interaction lengths even if we consider comparable phase errors at each DMZI

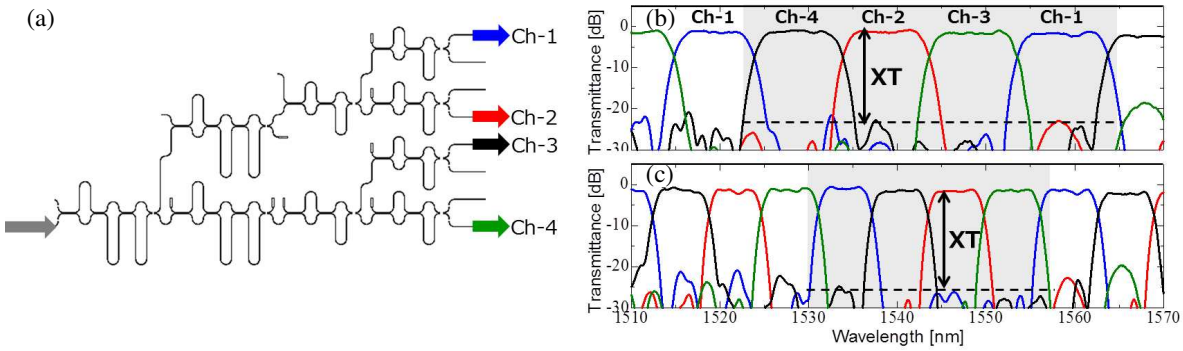

Figure 3: (a) Device configuration of 1×4Ch multistage DMZI-based DeMUX, and measured spectra with (b) $\Delta\nu = 10\,\text{nm}$ and (c) $\Delta\nu = 6.4\,\text{nm}$.

stage to the simple case. If the phase controllability of fabrication process far exceeds the degree of degradation by accumulated phase errors, we can count on spectral improvement in the device configuration shown in Fig. 3(a).

In this work, two kinds of $\Delta\nu$ were designed, fabricated and characterized. As shown in Figs. 3(b) and (c), irrespective of $\Delta\nu$, the DMZI-type device showed inter-channel-balanced flat-topped spectral response, together with low crosstalk of less than $-22\,\text{dB}$ for all output channels. These high performances resulted from good phase controllability enough to sustain desired spectral response within each DMZI by utilizing 300-mm wafer-scale ArF-immersion lithography process [8].

Finally, we experimentally evaluated spectral uniformity between inter-dies. In this experiment, the same multiple patterns equally spaced by $\sim 3\,\text{cm}$ were fabricated on a 300-mm SOI wafer. We characterized and compared DeMUX response of the devices located in the two nearest dies in the center of a 300-mm SOI wafer. As a result, the measured spectral characteristics including spectral shape, spectral flatness, insertion loss and crosstalk for the devices located in another die were almost the same as those shown in Figs. 4(b) and (c). Furthermore, the deviation of filtering wavelengths ($\delta\lambda$) was estimated to be $< 0.65\,\text{nm}$ for $\Delta\nu = 10\,\text{nm}$ and $< 0.5\,\text{nm}$ for $\Delta\nu = 6.4\,\text{nm}$, in spite of the fabrication imperfections and Si-core layer non-uniformity of the SOI wafer. That is, $\delta\lambda$ was ~ 10 times smaller than the 0.5 dB flat-topped bandwidths of 6.7 nm ($\Delta\nu = 10\,\text{nm}$) and 4.7 nm ($\Delta\nu = 6.4\,\text{nm}$), which justifies 300-mm ArF-immersion lithography process would be a promising technique for realizing several kinds of WDM photonic integrated devices with good production yields.

4. CONCLUSION

We reported recent progress of higher-order CROW and delayed interferometer type optical DeMUX fabricated by 300-mm SOI technology for WDM applications. High precision fabrication technology based on 300-mm wafer-scale ArF-immersion lithography process was proven to be very promising to realize several kinds of WDM filter devices together with good production yields.

ACKNOWLEDGMENT

This research is partly supported by New Energy and Industrial Technology Development Organization (NEDO). The authors would like to thank TIA-Super Clean Room Management Office, AIST, and especially M. Seki, N. Yokoyama, M. Ohtsuka, and K. Koshino for technical support and device fabrication. The authors also thank PETRA staffs and particularly T. Mogami, T. Horikawa, D. Shimura, T. Simoyama, S. Tanaka, M. Okuno and S. Okumura for valuable discussions.

REFERENCES

1. Miller, D. A. B., "Device requirements for optical interconnects to silicon chips," *IEEE Proceedings*, Vol. 97, No. 7, 1166–1185, 2009.
2. Liu, A., L. Liao, Y. Chetrit, J. Basak, H. Nguyen, D. Rubin, and M. Paniccia, "Wavelength division multiplexing circuit on silicon-on-insulator platform," *IEEE J. Sel. Top. Quantum Electron.*, Vol. 16, No. 1, 23–32, 2010.
3. Feng, N., S. Liao, D. Feng, P. Dong, D. Zheng, H. Liang, R. Shafiiha, G. Li, J. E. Cunningham, A. V. Krishnamoorthy, and M. Asghari, "High speed carrier-depletion modulators with 1.4 V-

cm $V_\pi L$ integrated on 0.25 μm silicon-on-insulator waveguides," *Opt. Express*, Vol. 18, No. 8, 7994–7999, 2010.

4. Kim, D. J., J. M. Lee, J. H. Song, J. Pyo, and G. Kim, "Crosstalk reduction in a shallow-etched silicon nanowire AWG," *IEEE Photon. Technol. Lett.*, Vol. 20, No. 19, 1615–1617, 2008.
5. Jeong, S.-H., S. Tanaka, T. Akiyama, S. Sekiguchi, Y. Tanaka, and K. Morito, "Flat-topped and low loss silicon-nanowire-type optical MUX/DeMUX employing multi-stage microring resonator assisted delayed Mach-Zehnder interferometers," *Opt. Express*, Vol. 20, No. 23, 26000–26011, 2012.
6. Selvaraja, S. K., G. Murdoch, A. Milenin, C. Delvaux, C. Ong, S. Pathak, D. Vermeulen, G. Stercks, G. Winroth, P. Verheyen, G. Lepage, W. Bogaerts, R. Baets, J. V. Campenhout, and P. Absil, "Advanced 300-mm wafer scale patterning for silicon photonics devices with low record loss and phase error," *Proc. OECC 2012*, PDP2-2, 2012.
7. Jeong, S.-H., D. Shimura, T. Simoyama, M. Seki, N. Yokoyama, M. Ohtsuka, K. Koshino, T. Horikawa, Y. Tanaka, and K. Morito, "Low-loss, flat-topped and spectrally uniform silicon-nanowire-based 5th-order CROW fabricated by ArF-immersion lithography process on a 300-mm SOI wafer," *Opt. Express*, Vol. 21, No. 25, 30163–30174, 2013.
8. Jeong, S.-H., D. Shimura, T. Simoyama, T. Horikawa, Y. Tanaka, and K. Morito, "Delayed interferometer based Si-wire WDM demultiplexers fabricated by phase controllable and productive 300-mm wafer-scale ArF-immersion lithography technology," *Proc. OFC 2014*, Th3F.5, 2014.
9. Kim, D. W., A. Barkai, R. Jones, N. Elek, H. Nguyen, and A. Liu, "Silicon-on-insulator eight-channel optical multiplexer based on a cascade of asymmetric Mach-Zehnder interferometers," *Opt. Lett.*, Vol. 33, No. 5, 530–532, 2008.
10. Horst, F., W. M. J. Green, S. Assefa, S. M. Shank, Y. A. Vlasov, and B. J. Offrein, "Cascaded Mach-Zehnder wavelength filters in silicon photonics for low loss and flat pass-band WDM (de-)multiplexing," *Opt. Express*, Vol. 21, No. 10, 11652–11658, 2013.
11. Assefa, S., S. Shank, W. Green, M. Khater, E. Kiewra, C. Reinholm, S. Kamlapurkar, A. Rylyakov, C. Schow, F. Horst, H. Pan, T. Topuria, P. Rice, D. M. Gill, J. Rosenberg, T. Barwicz, M. Yang, J. Proesel, J. Hofrichter, B. Offrein, X. Gu, W. Haensch, J. Ellis-Monaghan, and Y. Vlasov, "A 90 nm CMOS integrated nano-photonics technology for 25 Gbps WDM optical communications applications," *Proc. IEDM 2012*, 33.8, 2012.